Journal of Sulfur Chemistry
Publication details, including instructions for authors and subscription information:
http://www.informaworld.com/smpp/title~content=t713926081

Synthesis, spectral and structural study of sulfur-containing copper(II) complexes

R. N. Patel[a]; A. Singh[a]; K. K. Shukla[a]; D. K. Patel[a]; V. P. Sondhiya[a]; S. Dwivedi[a]
[a] Department of Chemistry, A.P.S. University, Rewa, Madhya Pradesh, India

Online publication date: 12 August 2010

To cite this Article Patel, R. N. , Singh, A. , Shukla, K. K. , Patel, D. K. , Sondhiya, V. P. and Dwivedi, S.(2010) 'Synthesis, spectral and structural study of sulfur-containing copper(II) complexes', Journal of Sulfur Chemistry, 31: 4, 299 — 313
To link to this Article: DOI: 10.1080/17415993.2010.499567
URL: http://dx.doi.org/10.1080/17415993.2010.499567

Journal of Sulfur Chemistry
Vol. 31, No. 4, August 2010, 299–313

Taylor & Francis
Taylor & Francis Group

Synthesis, spectral and structural study of sulfur-containing copper(II) complexes

R.N. Patel*, A. Singh, K.K. Shukla, D.K. Patel, V.P. Sondhiya and S. Dwivedi

Department of Chemistry, A.P.S. University, Rewa, Madhya Pradesh, India

(*Received 31 March 2010; final version received 5 June 2010*)

A series of four new copper(II) complexes $[Cu(H_2L)(L^1)]$ **1**, $[Cu(H_2L)(PMDT)]$ **2**, $[Cu(H_2L)(Dien)]$ **3** and $[Cu(H_2L)(L^2)]$ **4** have been synthesized by template condensation (H_2L = thiodiglycolic acid, L^1 = *N*-[(1)-1-(4-methylphenyl)ethylidene]benzohydrazide, PMDT = *N*,*N*,*N*′,*N*′,*N*″-pentamethyldiethylenetriamine, Dien = diethylenetriamine L^2 = *N*-[(1)-pyridin-2-ylmethylidene]benzohydrazide). The bonding and stereochemistry of the complexes have been characterized by molar conductance, elemental analysis, magnetic susceptibility, infrared, UV–visible, electron paramagnetic resonance structural studies and electrochemical studies. *g*-Values were calculated for all complexes in polycrystalline form as well as in DMSO solution. The magnetic and spectral data indicate square pyramidal geometry for **1** and octahedral geometry for **2**–**4** complexes. Cyclic voltammograms for all the complexes are similar and involve two irreversible redox processes. Their biological properties have also been studied. The thio complexes show more antibacterial activity than the controlled one. The antibacterial activities of the compounds have also been tested against *Escherichia coli* with different concentrations.

Keywords: copper(II) complexes; antibacterial activity; SOD activity; EPR; CV

1. Introduction

Copper is an essential element for life, as it actively participates in biological events (*1*). This transition metal is the second important element involved in the electron transfer process (*2–4*) and copper ions present in proteins play a crucial role as electron carrier in many vital processes. The large family of copper proteins includes one group of particular interest, the so-called type-1 or "blue" copper protein (TlCu). A number of publications, either experimental or theoretical, have been devoted to TlCu proteins, due to their special features such as their ability to transport electrons over large distances and hence to catalyze selected chemical reactions. Copper protein possess well-designed active centers that finally tune metal ion redox properties (*5*, *6*).

Thiodiglycolic acid and its metal complexes have received considerable attention over the past few years. The chemistry of such ligands warrants further study because thiodiglycolic acid forms an interesting series of copper(II) complexes with the help of other tridentate/bidentate ready-made ligands/Schiff base ligands. Some of the metal complexes may be expected to be biologically

*Corresponding author. Email: rnp64@ymail.com

ISSN 1741-5993 print/ISSN 1741-6000 online

DOI: 10.1080/17415993.2010.499567
http://www.informaworld.com

active. Indeed, carcinogenic activities (*7*) have already been found for some metal complexes of thiodiglycolic acid. The synthesis of these complexes continues to be of interest in order to evaluate their coordination chemistry and their potential as antimicrobial and anti-cancer agents.

In the present work, we describe four low molecular weight copper(II) complexes of thiodiglycolic acid focussing on their possible application as a superoxide scavenging agent. The ability of these copper(II) complexes to scavenge O_2^- was evaluated by NBT method. Spectroscopic studies were performed in order to correlate the structure feature of the complexes with their scavenging activity.

2. Results and discussion

H_2L forms square pyramidal **1** and octahedral complexes **2**–**4** with $Cu(NO_3)_2 \cdot 3H_2O$ in methanol. All the complexes were synthesized by the following sequential route (Scheme 1).

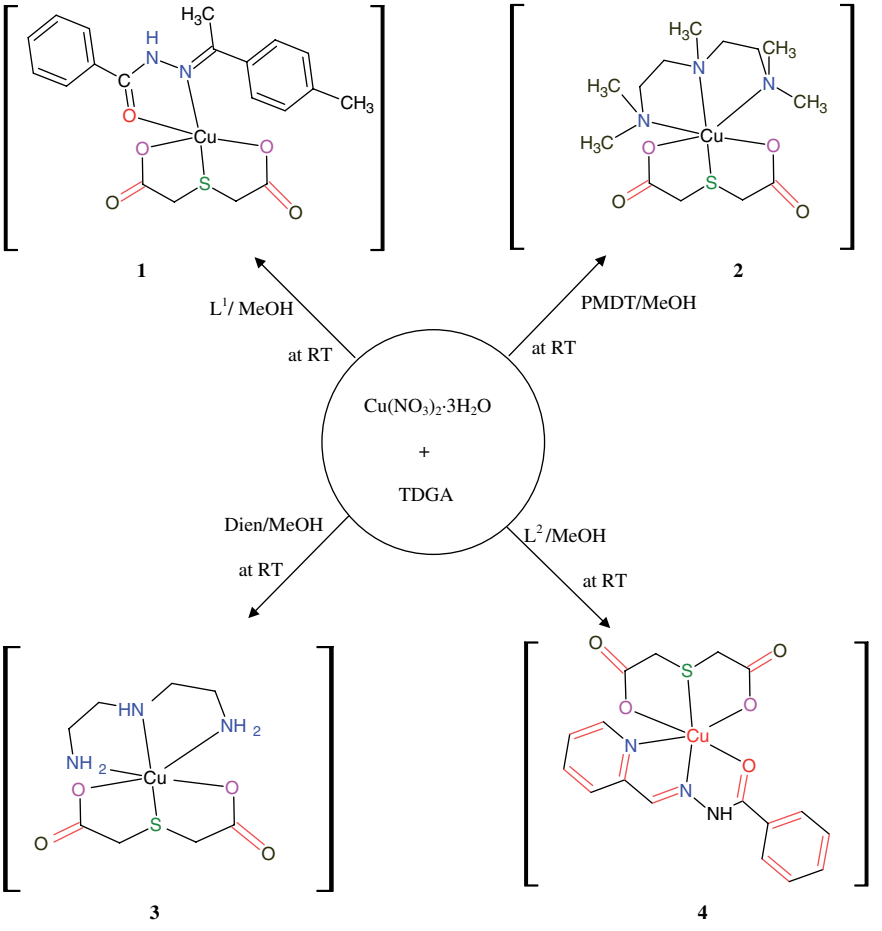

Scheme 1. Synthesis of complexes **1**–**4**.

All the copper(II) complexes are hygroscopic in nature. These are insoluble in common organic solvents but soluble in DMF and DMSO. The elemental analysis shows that the copper(II)

Table 1. The important IR frequencies (in cm^{-1}) of Schiff bases and their metal complexes.

Compound	ν(OH)	ν(C–O)	ν(C=O)	ν(C=N)	ν(C–S)	ν(N–H)	ν(NH_2)	ν (Cu–N_{py})	ν(Cu–N)	ν(Cu–O)	ν(Cu–S)
H_2L	3060	1106	1650		1324	–	–	–	–	–	–
L^1	–	–	1632	1558	–	3273	–	–	–	–	–
L^2	–	–	1635	1560	–	3274	–	–	–	–	–
1	–	–	1630	1580	1338	3260		–		525	350
2	–	–	1635	–	1337	3268	3385	–	465	520	353
3	–	–	1625	–	1336	3265	3370	–	460	526	352
4	–	–	1630	1582	1331	3266	–	280	463	520	349

complexes have non-stoichiometric ratio of the type [M(H_2L)(A)], where H_2L stands for a sulfur donor ligand containing SO_2-bonding moiety. Several attempts were made to develop the single crystal of the complexes but failed due to the insolubility of the complexes in common organic solvents. All the complexes are non-electrolytic in nature.

2.1. *Infrared spectral studies*

The important IR spectral data of Schiff bases and their Cu(II) complexes are presented in Table 1. The free ligand displays a broad band at 3030–3065 cm^{-1} due to O–H vibrations of the alcoholic hydroxyl oxygen. This band disappears in the spectra of complexes indicating that the ligand is coordinated to metal through deprotonated form (*8*). The ring vibrations and C–O stretching modes of the ligand appear in the 1440–1513 and 1100–1190 cm^{-1} ranges, respectively. In the spectra of complexes, these bands shift to higher wavenumbers as a result of coordination through the hydroxyl oxygen atoms. A strong band in the region 1558 and 1560 cm^{-1} in the free ligands (L^1 and L^2) assigned to (N=C-CH_3) exhibits $\pm$10–20 cm^{-1} shifting (*9–11*) in the spectra of complexes (**1** and **4**) indicating (*12*) coordination through azomethine nitrogen of Schiff bases. This can be explained by the donation of electrons from nitrogen to the empty d-orbitals of the central metal atom. Formation of M–$N_{(azo)}$ bond (*12*) is further supported by the presence of a band in the region 460–465 cm^{-1}. A new band appearing at $\sim$750 cm^{-1} which is assigned to C–S indicates the coordination through the sulfur atom in these complexes. Metal–sulfur bond formation (*13–15*) is further confirmed by a band in the region 349–353 cm^{-1} in the far IR spectra and confirms the complexation. The IR spectra of the ligand H_2L shows characteristic bands due to C–S and C=O in the regions 1324 and 1650 cm^{-1}, whereas NH stretching absorption in free ligands (L^1 and L^2) occurs at $\sim$3273 cm^{-1} (*16, 17*). The N–H vibration bands of the complexes **1**, **3** and **4** are observed between 3260–3268 cm^{-1}. In the complexes, these bands are shifted to lower wavenumbers, indicating the involvement of nitrogen atoms in coordination. This is also confirmed by the presence of new bands at 500–581 cm^{-1} in the spectra of complexes corresponding to N–N vibration bands (*18*). In complex **4**, a strong band is observed in the region 280 cm^{-1}, which is consistent with the Cu–N of pyridine suggested by Clark and Williams (*19*). In all the complexes, a strong band is observed in the region 349–353 cm^{-1}, which has been assigned to the Cu–S band (*20*).

2.2. *Electronic spectra*

It has been established that six coordinate copper(II) complexes possess elongated tetrahedral or rhombic distortions in an octahedral field and display three spin allowed transitions (Figure 1) assigned to $^2B_{1g} \rightarrow {}^2B_{1g}$ (ν_1), $^2B_{1g} \rightarrow {}^2B_{2g}$ (ν_2) and $^2B_{1g} \rightarrow {}^2E_g$ (ν_3) absorption (*21, 22*). However, the first transition usually appears as shoulder and sometimes overlaps with the later transition (ν_2). The complexes **1–4** exhibited three bands around 15,050–26,400 cm^{-1}. The broadness of

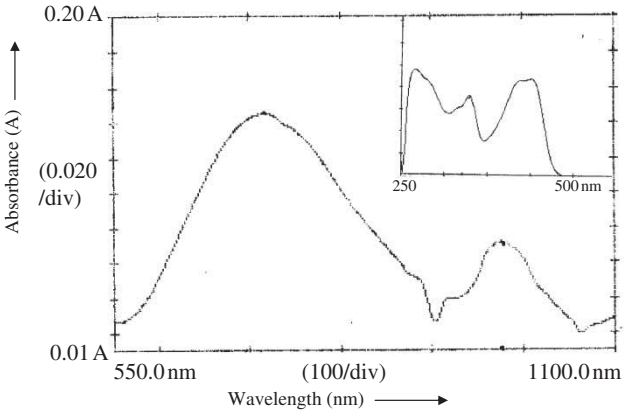

Figure 1. The UV–visible spectrum (0.003 mol^{-1} dm^{-3}) of complex **4**.

band is due to ligand-field and the John-Teller distortions (*23*). Additional bands observed for all complexes in the range 25,000–27,777 cm^{-1} are assigned to S→Cu transition (*24*, *25*).

2.3. *Magnetic moment studies*

The magnetic susceptibility measurements for complexes **1**–**4** were measured in the solid state. They showed the paramagnetic behavior at room temperature. The observed magnetic moments of these complexes are quite close to the value expected for other copper(II) complexes. The magnetic moment value (μ_{eff}) of complexes **1**–**4** are 1.89, 1.87, 1.88 and 1.91 B.M., respectively. Magnetic moment values lie within the range normally found for other magnetically dilute copper(II) complexes (*26*–*28*).

2.4. *Molar conductivity*

The molar conductance values of the compounds **1**–**4** were measured in DMSO solution (3×10^{-3} M). On the basis of observed values, the complexes are found to be nonconductors (*29*) which indicates that the anionic ligand is coordinated to the central copper(II).

2.5. *Electron paramagnetic resonance spectra*

The powder and solution spectra of complexes showed $g_{\parallel}$ and $g_{\perp}$ patterns only, and the corresponding values (∼2.0) were found to be consistent with the distorted octahedral coordination (*30*) around copper(II) in complexes **2**–**4** with the $d_{x^2-y^2}$ ground state (*31*). However, superhyperfine splitting is only observed in complex **4**, whereas it could not be observed in the rest of the complexes. The spectra of **4** have five nitrogen superhyperfine lines on the high-field copper hyperfine splitting component, which arises from the coupling of the electron spin with the nuclear spin of the two nitrogen atoms, *i.e.* one azomethine nitrogen and one nitrogen from the pyridine ring coordinated to the copper(II) center (Figure 2).

The electron paramagnetic resonance (EPR) spectra of a polycrystalline sample at 298 K were recorded in the X band using the 100 kHz field modulation, and g-factors were quoted relative to the standard marker TCNE ($g = 2.00277$). The frozen solution EPR spectra and polycrystalline sample EPR spectra are shown in Figures 2–5. The derived EPR parameters for copper(II) complexes are presented in Table 2. The spectra of complex **4** in the polycrystalline state at 298 K

Table 2. EPR spectral parameters of the copper(II) complexes.

EPR parameters	**1**	**2**	**3**	**4**
Polycrystalline state (298 K)				
g_1	2.222	2.214	2.260	2.192
g_2	2.059	2.124	2.141	2.141
g_3	–	2.073	2.073	2.050
DMSO (77 K)				
$g_\parallel$	2.207	2.196	2.108	2.2184
$g_\perp$	2.050	2.012	2.050	2.059
$A_\parallel$ (G)	160	170	195	170
G	4.1	3.9	4.3	3.7
α^2	0.678	0.693	0.772	0.719
β^2	0.989	0.953	0.918	1.067
γ^2	0.947	0.948	0.881	1.016
$K_\perp$	0.648	0.657	0.680	0.731
$K_\parallel$	0.664	0.661	0.709	0.768
f(cm)	147	139	122	139

show only one broad signal isotropic, and hence only one g-value (2.0863) arises between different molecules in the unit cell. This is suggestive of the presence of spin–spin interaction, which may be the only intermolecular type arising due to the solid effect. These types of spectra unfortunately give no information on the electronic ground state of the copper(II) ion present in the complexes.

The low-temperature (77 K) DMSO-frozen glass EPR spectra of these complexes display four-line copper hyperfine lines, characteristic of monomeric copper(II) complexes with a $g_\perp$ component. Kivelson and Nieman (*32*) have pointed out that compounds having $g_\parallel > 2.3$ are ionic in nature while those with $g < 2.3$ are covalent in character. The $g_\parallel$ values for complexes **1**–**4** reveal appreciable covalency with $d_{x^2-y^2}$ as the ground state. The complexes show similar features with $g_\parallel > g_\perp$. It is interesting that the relationship $g_\parallel > g_\perp$ typical of axially symmetric d^9 copper ($S_{Cu} = \pm 1/2$) having unpaired $d_{x^2-y^2}$ orbital (*33*, *34*). Similar observations were made earlier (*35*) for mixed-ligand copper(II) complexes. The $g_\parallel$ value of the complexes is found to be $g_\parallel < 2.3$ which indicates considerable covalent character of the M→L bond (*36*). In complexes **1**–**4**, all EPR signals are shifted slightly towards higher magnetic field and therefore leading to smaller $g_\parallel$ and $g_\perp$ values. This finding is in line with the increased ligand field

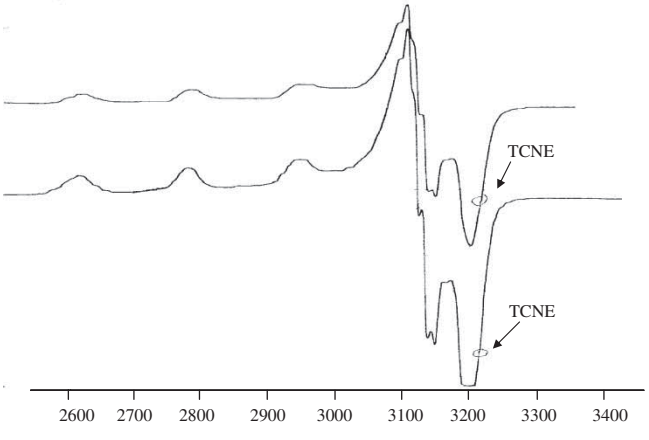

Figure 2. EPR spectra (LNT) of complex **4** in 100% DMSO.

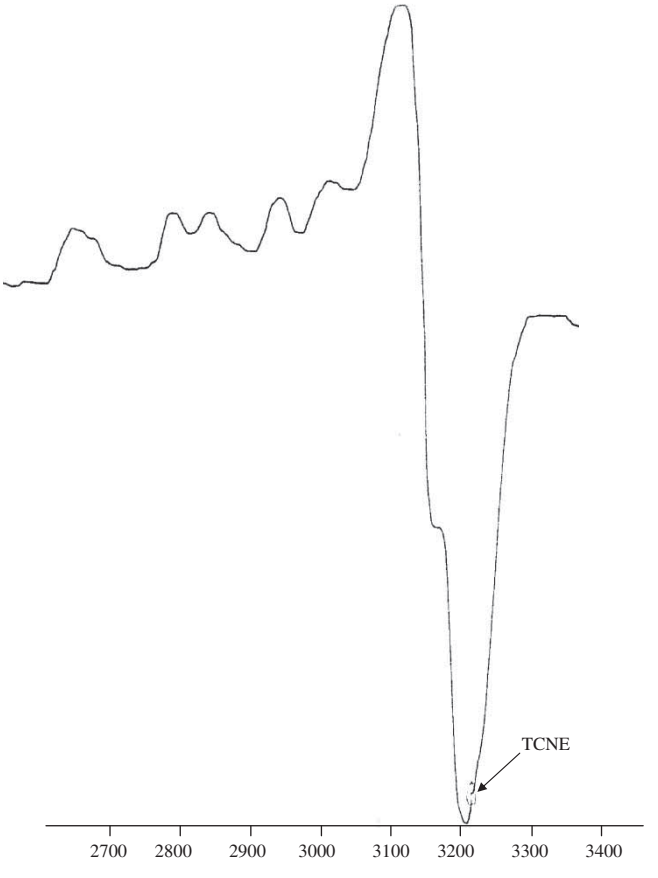

Figure 3. EPR spectra (LNT) of complex **3** in 100% DMSO.

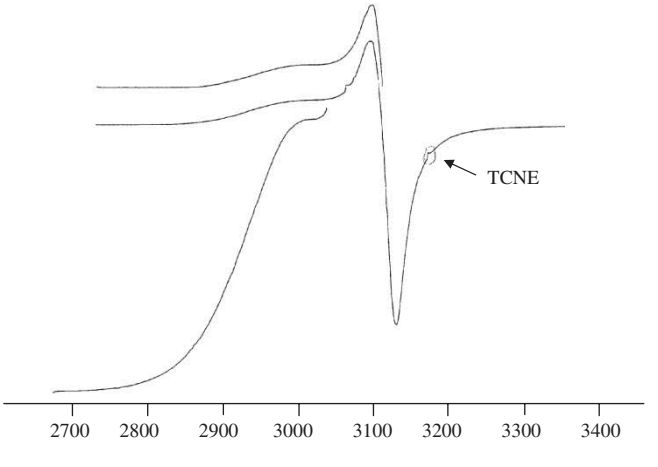

Figure 4. EPR spectrum of complex **1** in a polycrystalline state at RT.

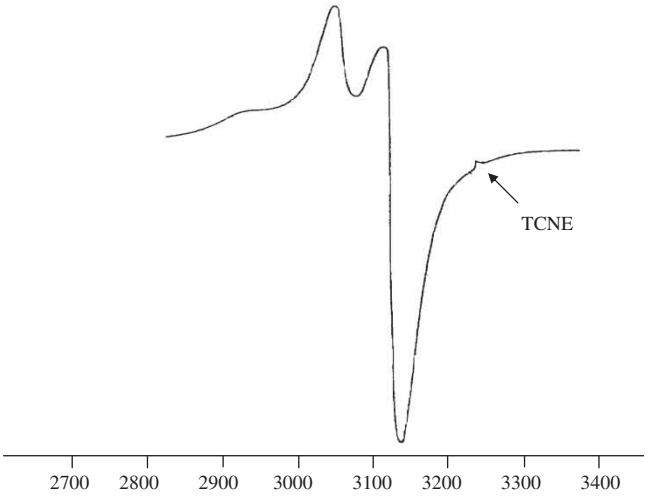

Figure 5. EPR spectrum of complex **2** in a polycrystalline state at RT.

operating through the $G = 2.0023 + n\xi\ [E^0 - En]$ relationship (*35*, *36*). The geometric parameter G, which is a measure of the exchange of interaction between the copper centers in a polycrystalline solid, has been calculated. According to Hathaway and coworkers (*37*, *38*), if $G > 4$, the exchange interaction is negligible and $G < 4$ indicates the exchange interaction. The value of G for complexes **1**–**4** are 4.1, 3.9, 4.3 and 3.7, indicating that exchange interaction is negligible for **1** and **3**, whereas complexes **2** and **4** show exchange interaction in solid state. From the low-temperature EPR spectra, various bonding parameters such as in-plane σ-bonding, in-plane π-bonding as well as out-of-plane π-bonding can be evaluated (*39*) by using the following expression (*40*)

$$\alpha^2 = \left(\frac{A_\parallel}{0.036}\right) + (g_\parallel - 2.0023) + \frac{3}{7}(g_\perp - 2.0023) + 0.04.$$

The orbital reduction factors $K_\parallel$ and $K_\perp$ were estimated from the expression (*40*)

$$K_\parallel^2 = (g_\parallel - 2.0023)\frac{E_{d-d}}{8\lambda_0},$$

$$K_\perp^2 = (g_\perp - 2.0023)\frac{E_{d-d}}{2\lambda_0},$$

where $K_\parallel = \alpha^2\beta^2$, $K_\perp = \alpha^2\gamma^2$ and λ_0 represents the one-electron spin–orbit coupling constant for the free ion, equal to $-828\,\mathrm{cm}^{-1}$. Significant information about the nature of bonding in the copper(II) complexes can be derived from the magnitude of $K_\parallel$ and $K_\perp$. In the case of pure σ-bonding, $K_\parallel \approx K_\perp \approx 0.77$, whereas $K_\parallel < K_\perp$ implies considerable in-plane bonding, and for out-of-plane bonding, $K_\parallel > K_\perp$. In all the present copper(II)complexes, it is observed that $K_\parallel > K_\perp$, which indicates the presence of a significant out-of-plane bonding. The evaluated values of α^2, β^2 and γ^2 of the complexes are consistent with both strong in-plane σ- and in-plane π-bonding. The computed values of α^2 and β^2 (Table 2) are compared with those of other copper(II) complexes which are ionic in nature (*41*). Therefore, the present complexes may be regarded as ionic complexes. The f-values of these complexes are found to be 147 for **1**, 139 for **2**, 122 for **3** and 139 for **4**, indicating significant distortion from planarity.

2.6. *Cyclic voltammetry*

The cyclic voltammogram for copper(II) complexes exhibit a metal-centered electrochemical process. All the copper(II) complexes show a similar electrochemical behavior. The cyclic voltammogram (Figure 6) of the representative complex is discussed here. The representative cyclic voltammogram and relative parameter are given in Figure 6 and Table 3. Inspection of this figure indicates that the reduction wave (Peak B) and its oxidation counterpart (Peak C) are related to the Cu(II)/Cu(I) reduction process in the range 0 to -1.4 V while on the anodic side (range 0 to $+1.2$ V), there exists an oxidation curve (Peak D) with its cathodic peak (Peak A). Analysis of the cyclic voltammetric response of peak B/C indicates that this process originates from an irreversible Cu(II)/Cu(I) redox couple with a peak-to-peak separation (ΔE_p) of more than 350 mV and the ratio of I_{pa}/I_{pc} is also more than unity. It is expected that the Cu(II)/Cu(I) couple experiences some structural reorganization barrier while undergoing the reduction process. Patterson and Holm (*42*) have shown that softer ligands tend to favor more positive $E_{1/2}$ values while hard acids give rise to more negative values.

The cyclic voltammetric behavior of all complexes between -0.250 to $+1.2$ V shows cathodic response with its oxidation counterpart in the range -0.250 to -0.325 V. This feature corresponds to an irreversible couple Cu(III)/Cu(II) process (*43*), as indicated by ΔE_p values. The redox process associated with the oxidation of Cu(II) to Cu(III) may probably originate due to the presence of the thio center. During the reverse scan, the oxidation of Cu(I)/Cu(II) skips over and passes to the Cu(III) state. This was confirmed by the ratio of the anodic to the cathodic current value of the Cu(II)/Cu(III) couple ($I_{pa}/I_{pc} = 2$). Since the thiodiglycolic acid is a flexible ligand, it can adopt different conformations so as to fit the smaller size Cu(III) ion, thus favoring the oxidation process. Moreover, this oxidation step results in the formation of a low-spin d^8 Cu(III) state with a preference for a square planar geometry (*44*).

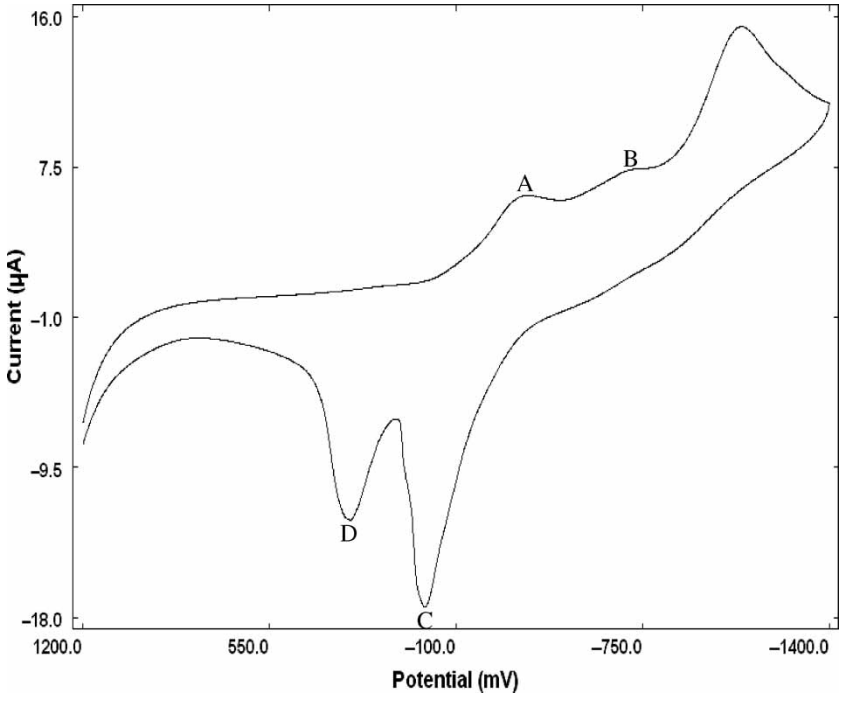

Figure 6. Cyclic voltammogram of complex **2** in DMSO (0.1 M $NaClO_4$ as the supporting electrolyte, scan rate: 100 mV/s).

Table 3. Cyclic voltammetric data for 1 mM solution of the Cu(II) complexes in DMSO containing 0.1 M $NaClO_4$ as supporting electrolytes.

Compound	Scan rate	E_{pc} (mV)	I_{pc} (μA)	E_{pa} (mV)	I_{pa} (μA)	ΔE_p (mV)	$E^{0'}$ (mV)	$I_{pa}/I_{pc}(\mu A)$
1	100	−284	0.979	275	1.958	559	−4.5	2.0
	200	−308	1.379	318	2.771	626	−5.0	2.0
	300	−320	2.142	336	4.348	656	−8.0	2.0
2	100	−301	4.3965	239	8.880	540	−31	2.0
	200	−363	6.624	285	13.446	648	−39	2.0
	300	−394	7.558	324	15.040	718	−35	1.9
3	100	−344	2.606	−40	5.290	−304	−152	2.0
	200	−350	2.789	−12	5.8569	−338	−169	2.1
	300	−358	3.802	31	7.718	−327	−163	2.0
4	100	275	1.944	351	3.907	75	313	2.0
	200	253	4.913	373	9.727	119	313	1.9
	300	231	6.296	395	12.654	164	313	2.0

Note: $\Delta E_p = E_{pa} - E_{pc}$; $E^{0'} = (E_{pa} + E_{pc})/2$.

2.7. *SOD activity*

The SOD-like activities of all the complexes were investigated by NBT assay, and the catalytic activity toward the dismutation of superoxide ion was measured. The coordination arm with two hydroxyethyl arms provide a stable and flexible environment similar to that in the active sites of the native enzymes, insuring the stable existence of the native enzyme and the stable existence of the complexes. In this work, the SOD-like activities for the four complexes were measured.

The chromophore concentration required to yield 50% inhibition of the reduction of NBT(IC_{50}) was determined by the following literature method (*45*). The representative graph showing IC_{50} value for complex **1** is given in Figure 7. The IC_{50} data of the SOD activity assay along with kinetic catalytic constants of **1**–**4** complexes (*46*, *47*) are presented in Table 4. The IC_{50} values for complexes **1**–**4** are 44, 59, 53 and 65 μM, respectively. The activities of these complexes are similar to those of the other mononuclear complexes (*48–50*). They are among the most active model compounds but are somewhat less active than the native enzyme ($IC_{50} = 0.04\,\mu M$).

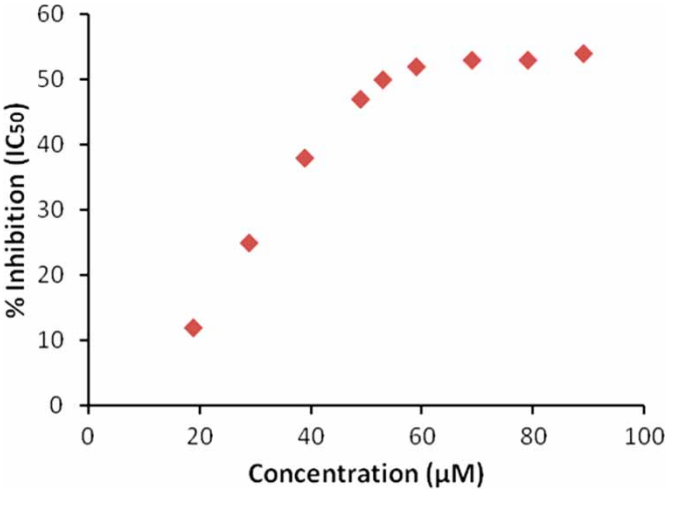

Figure 7. SOD activity of **1**.

Table 4. IC_{50} values and kinetic constant of **1–4**.

Compound	IC_{50} (μmol)	$k_{McCF}(M^{-1}\,s^{-1})^b \times 10^4$
1	44	2.16
2	59	1.61
3	53	1.79
4	65	1.46

Note: k_{McCF} were calculated by $K = k_{NBT} \times [NBT]/IC_{50}$, k_{NBT} (pH 7.8) $= 5.94 \times 10^4\,M^{-1}\,s^{-1}$ (*46*, *47*).

Figure 8. A representative photograph of the size of inhibition diameter of control against *E. coli* bacteria.

Figure 9. A representative photograph of the size of inhibition diameter of **2** against *E. coli* bacteria.

The difference in IC_{50} values for the complexes should be ascribed to the evident discrepancy in the structures between them, especially in the confirmation of the ligand. Especially the two labile hydroxyl arms, which are proposed to be easily substituted by the substrate, O_2^-, in the catalytic process, just like the O_2^- in place of the water molecule bound to the copper site in the mechanism of dismutation of superoxide ion by native SOD.

2.8. *Antimicrobial activity*

The biological and medicinal potency of coordination compounds has been established in their antitumor, antiviral and antimalarial activities. This characteristic property has been related to the ability of the metal ion to form complexes with a ligand containing sulfur and oxygen donor atoms. The synthesized ligands and their complexes were screened for their antibacterial activity

Table 5. Antibacterial results of Schiff base and their metal complexes.

Compound	Concentration ($\mu g/l$)	Diameter of inhibition zone (in mm) *E. coli*
$\mathbf{L}^1$	0.003	1
$\mathbf{L}^2$	0.003	1
1	0.001	1
	0.002	Not clear inhibition zone
	0.003	2
2	0.001	3
	0.002	3
	0.003	5
3	0.001	1
	0.002	1
	0.003	3
4	0.001	Not clear inhibition zone
	0.002	2
	0.003	3
DMSO (control)		No inhibition zone

Note: Key to interpretation (for 100 μg/l): less than 12 mm, inactive; 12–16 mm, moderately active; above 16 mm, highly active.

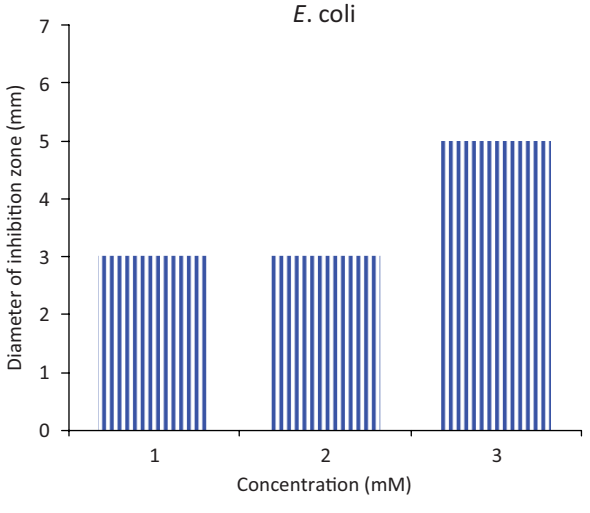

Figure 10. Antibmicrobial activity of complex **2**.

(*51*) against *Escherichia coli*. Their activity was determined by measuring the diameter of zone of inhibition (in mm) (Figures 8 and 9, Table 5). All the complexes showed a high antibacterial activity against *E. coli* (Figure 10). In particular, all complexes showed higher activity than the respective Schiff bases. This higher activity of the metal complexes compared with the Schiff bases may be due to the change in the structure due to coordination.

3. Conclusion

The elemental analysis, magnetic susceptibility and electronic, IR and ESR spectral observations suggest the square pyramidal geometry for the complex **1** and an octahedral geometry for complexes **2**–**4**. They show a high antibacterial activity against *E. coli*.

4. Experimental

4.1. *Materials*

Copper(II) nitrate trihydrate was purchased from S.D. Fine Chemicals, India. All other chemicals used were of synthetic grade and used without further purification.

4.2. *Synthesis of Schiff base* L^1

The Schiff base was prepared by the reaction of 4-methylacetophenone and benzoylhydrazine (Scheme 2). A solution of 4-methylacetophenone (2.70 g, 20.0 mmol) in ethanol (10 ml) was mixed with the stirred solution of benzoylhydrazine (2.70 g, 20.0 mmol). The resulting solution was refluxed for 4 h after the addition of one to two drops of acetic acid. On cooling the solution at room temperature, pale yellow crystals were separated, filtered and washed with methanol. The product was recrystallized in high yield from hot ethanol. Yield: 4.136 g (88%). Anal. Calcd for $C_{16}H_{16}N_2O$: C, 76.16; H, 6.39; N, 11.10%. Found: C, 76.06; H, 6.25; N, 11.02%. FAB Mass (m/z) Found: 251.95, Calcd: 252.31.

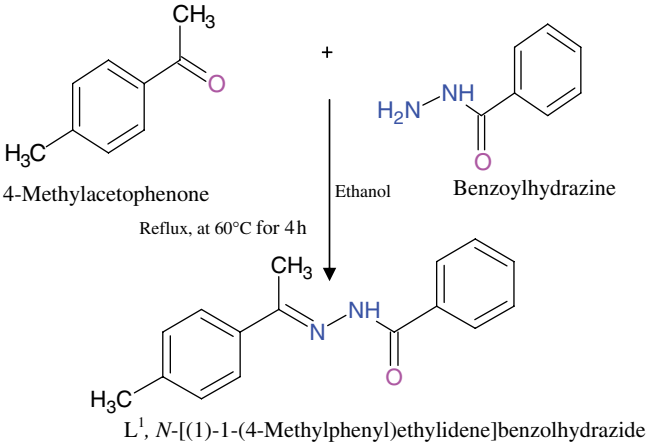

L^1, *N*-[(1)-1-(4-Methylphenyl)ethylidene]benzolhydrazide

Scheme 2. Synthesis of ligand L^1.

4.3. *Synthesis of Schiff base* L^2

N-[(1)-Pyridin-2-ylmethylidene]benzohydrazide was prepared according to the method reported (*52*) in the literature. L^1 was synthesized by reacting benzohydrazide and 2-pyridenecarboxaldehyde in ethanol. Yield 2.06 g (85%). Anal. Calcd for $C_{13}H_{11}N_3O$: C, 69.25; H, 4.88; N, 18.64%. Found: C, 69.02; H, 4.56; N, 18.45%. FAB mass (*m*/*z*) calcd: 225.26. Found: 225.26. Details of the synthesis are described as the supporting information in Scheme 3.

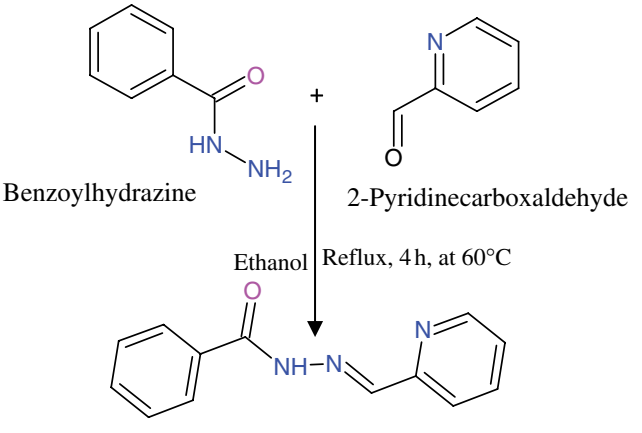

L^2 *N*-[(1)-Pyridin-2-ylmethylidene]benzohydrazide

Scheme 3. Synthesis of ligand L^2.

4.4. *Synthesis of* $[Cu(H_2L)(L^1)]$ *(1)*

To a methanolic solution (10 ml) of cupric nitrate trihydrate (1.0 mmol, 0.241 g), a solution of L^1 (1.0 mmol, 0.252 g) in methanol was added with constant stirring at room temperature for 30 min. After 1 h of stirring, a methanolic solution (10 ml) of thiodiglycolic acid (1.0 mmol, 0.116 g) was added. The resultant solution was stirred for 4 h. The solution was filtered and allowed to stand at room temperature for a few days. The brownish sticky complex was collected and stored in a $CaCl_2$ desiccator. Yield 0.481 g (79%). Anal. Calcd for $C_{19}H_{20}CuN_2SO$ (**1**): C, 52.7; H, 4.63; N, 6.48%. Found: C, 51.89; H, 3.98; N, 5.98%. FAB mass (*m*/*z*) found: 432.0. Calcd: 431.88.

4.5. *Synthesis of* $[Cu(H_2L)(PMDT)]$ *(2),* $[Cu(H_2L)(Dien)]$ *(3) and* $[Cu(H_2L)(L^2)]$ *(4)*

Complexes **2**–**4** were synthesized following the same procedure as **1**, only PMDT (1.0 mmol, 0.173 g) for **2**, Dien (1.0 mmol, 0.103 g) for **3** and L^2 (1.0 mmol, 0.225 g) for **4** were added. The resultant solution was stirred for 4 h. The solution was filtered and allowed to stand at room temperature for a few days. The brownish sticky complex was collected and stored in a $CaCl_2$ desiccator. Yield 0.435 g (82%). Anal. Calcd for $C_{12}H_{27}CuN_3S$ (**2**): C, 40.70; H, 7.63; N, 11.89%. Found: C, 40.55; H, 7.45; N, 11.67%. FAB mass (*m*/*z*) found: 353.3. Calcd: 351.89. Yield 0.368 g (80%). Anal. Calcd for $C_7H_{17}CuN_3S$ (**3**): C, 29.67; H, 6.01; N, 14.83%. Found: C, 29.45; H, 5.85; N, 14.55%. FAB mass (*m*/*z*) found: 283.17. Calcd: 282.86. Yield 0.480 g (84%). Anal. Calcd for $C_{16}H_{15}CuN_3SO$ (**4**): C, 47.37; H, 3.70; N, 10.36%. Found: C, 46.89; H, 3.65; N, 10.95%. FAB mass (*m*/*z*) found: 405.26. Calcd: 404.86.

4.6. *Physical measurements*

Elemental analyses of the complexes were performed on an Elementar Vario EL III Carlo Erba 1108 analyser. FAB mass spectra were recorded on a JEOL SX 102/DA 6000 mass spectrometer/data system using xenon (6 kV, 10 mA) as the FAB gas. The accelerating voltage was 10 kV and the spectra were recorded at room temperature. UV–visible spectra were recorded at 298 K on a Shimadzu UV–visible recording spectrophotometer UV-160 in quartz cells. IR spectra were recorded in a KBr medium on a Perkin-Elmer spectrophotometer. X-band EPR spectra were recorded with a Varian E-line Century Series Spectrometer equipped with a dual cavity and operating at X-band (~9.4 GHz) with a 100 kHz modulation frequency. TCNE was used as a field marker. The frozen solutions at liquid nitrogen temperature used for EPR spectra were in 3×10^{-3} M DMSO solution. The Varian quartz tubes were used for measuring EPR spectra of polycrystalline samples and frozen solutions. The EPR parameters for copper(II) complexes were determined accurately from a computer simulation program (*53*). Magnetic susceptibility measurements were made on a Gouy balance using a mercury(II) tetrathiocyanato cobaltate(II) as the calibrating agent ($\chi_g = 16.44 \times 10^{-6}$ cgs units). Cyclic voltammetry was carried out with a BAS-100 Epsilon electrochemical analyzer having an electrochemical cell with a three-electrode system. Ag/AgCl was used as a reference electrode, glassy carbon as a working electrode and platinum wire as an auxiliary electrode; 0.1 M $NaClO_4$ was used as the supporting electrolyte and DMSO as the solvent. All measurements were carried out at 298 K under a nitrogen atmosphere. Molar conductivities of the freshly prepared 2×10^{-3} M DMSO solutions were measured on a Systronics conductivity TDS meter 308.

4.7. *In vitro antibacterial assay*

The *in vitro* antimicrobial (antibacterial) activities of these complexes were tested using the paper disk diffusion method (*54*). The chosen strain was *E. coli*. The liquid medium containing the bacterial subculture was autoclaved for 20 min at 121°C and at 15 lb pressure before inoculation. The bacteria were then cultured for 24 h at 36°C in an incubator. Nutrient agar was poured into a plate and allowed to solidify. The test compounds (DMSO solutions) were added dropwise to a 10 mm diameter filter paper disk placed at the center of each agar plate. The plates were kept at 5°C for 1 h and then transferred to an incubator maintained at 36°C. The diameter of the growth of inhibition zone around the disk was measured after 24 h incubation. Three replicates were made for each treatment.

Acknowledgements

Our grateful thanks are due to the National Single Crystal X-ray Diffraction Facility, X-ray Division and RSIC (SAIF), IIT Mumbai, for EPR measurements. The Head RSIC (SAIF), Central Drug Research Institute, Lucknow, is also thankfully acknowledged for providing analytical and spectral facilities. Financial assistance from UGC [Scheme no. 36-28/2008 (SR)] and DRDO [Scheme no. ERIP/Er/06357/M/01/1118], New Delhi, are also thankfully acknowledged.

References

(1) Malamstrom, B.G. *ZeitschriftfurNaturwissenschaFtlichmedizinische Grundlagen Forschung* **1965,** *2,* 259–266.
(2) Gray, H.B. *Proc. Natl Acad. Sci. USA* **2003,** *100,* 3563–3568.
(3) Finney, L.A.; O'Halloran, T.V. *Science* **2003,** *300,* 931–936.
(4) Cantars, G.W.; Dennision, C. *Biochimi.* **1995,** *77,* 506–515.
(5) Alcaraz, L.A.; Gomez, J.; Ramirez, P.; Carlvente, J.J.; Andreu, R.; Donaire, A. *BioInorg. Chem. Appl.* **2007,** *16,* 1–9.
(6) Paraskevopoulos, K.; Sundararajan, M.; Surendran, R. *J. Chem. Soc. Dalton Trans.* **2006,** *25,* 3067–3076.
(7) Majumder, S.M.M.H.; Ali, M.A.; Smith, F.E.; Mridha, M.A.U. *Polyhedron* **1988,** *7,* 2183–2187.

(8) Nakamoto, K. *Infrared Spectra of Inorganic and Coordination Compounds*, 2nd ed.; J. Wiley: New York, 1970; p 376.
(9) Gavr, S.; Sharma, B. *J. Indian Chem. Soc.* **2003,** *8*, 841–842.
(10) Daniel, T.T.; Natarajan, K. *Transition Met. Chem*. **2000,** *25*, 347–351.
(11) Sharma, B.D.; Bailar, J.C. *J. Am. Chem. Soc.* **1955,** *77*, 5476–5480.
(12) Singh, K.; Singh Barwa, M.; Tyagi, P. *Eur. J. Med. Chem.* **2006,** *41*, 147–153.
(13) Sengupta, S.K.; Pandey, O.P.; Shrivastava, A.K.; Rai, R.; Mishra, K.D. *Indian J. Chem. Sec. A* **1999,** *38*, 956–960.
(14) Verma, R.S.; Garg, P.K. *J. Indian Chem. Soc.* **1981,** *58*, 980–981.
(15) Sen, A.K.; Singh, G.; Singh, K.; Hunda, R.N.; Dubey, S.N. *Proc. Indian Acad. Sci.* (*Chem Sci.*) **1998,** *110*, 75–81.
(16) Singh, G.; Singh, D.A.; Singh, K.; Singh, D.P.; Hunda, R.N.; Dubey, S.N. *Proc. Indian Acad. Sci. Ind.* **2002,** *72A*, 87–94.
(17) Agrawal, R.K.; Sarin, R.K.; Agrawal, H. *Bull. Chem. Soc., Ethiopia* **1995,** *9*, 23–29.
(18) Nakamoto, K. *Infrared and Raman Spectra of Inorganic and Coordination Compound*, 5th ed.; J. Wiley: New York, 1997.
(19) Clark, R.J.; Williams, C.S. *Inorg. Chem.* **1965,** *4*, 350–357.
(20) Kumar, A.; Kulkarni, D.; Patil, S.A.; Badami, P.S. *J. Sufur Chem.* **2009,** *30*, 145–159.
(21) Chikate, R.C.; Padhye, S.B. *Polyhedron* **2005,** *24*, 1689–1700.
(22) Lever, A.B.P. *Inorganic Electronic Spectroscopy*, 2nd ed.; Elsevier: Amsterdam, 1984.
(23) Kneubunl, F.K. *J. Chem. Phys*. **1960,** *33*, 1074–1077.
(24) Ainscough, E.W.; Brodie, A.M.; Larsen, N.G. *Inorg. Chim. Acta* **1982,** *60*, 25–34.
(25) Dedert, P.L.; Thompson, J.S.; Ibers, J.A.; Marks, T.J. *Inorg. Chem.* **1982,** *21*, 969–977.
(26) Nonoyama, M.; Yamasaki, K. *Inorg. Chim. Acta* **1971,** *5*, 124–128.
(27) El-Shatzly, M.F.; EI-Dissowky, A.; Salem, T.; Osman, M. *Inorg. Chim. Acta* **1980,** *40*, 1–6.
(28) Patil, N.; Patil, B.R. *Oriental J. Chem*. **2002,** *18*, 547–550.
(29) Geary, W.J. *Coord. Chem. Rev.* **1971,** *7*, 81–122.
(30) Hathaway, B.J. In *Comprehensive Coordination Chemistry*: Wilkinson, G., Gillard, R.G., McCleverty, J.A., Eds.; Pergamon Press: Oxford, 1987; Vol. 5, p 533.
(31) Zoroddu, M.A.; Pilo, M.T.; Seeber, R.; Pogni, R.; Basosi, R. *Inorg. Chim. Acta* **1991,** *183*, 185–189.
(32) Kivelson, D.; Nieman, R. *J. Chem. Phys*. **1961,** *35*, 149–155.
(33) Patel, R.N.; Gundla, V.L.N.; Patel, D.K. *Polyhedron* **2008,** *27*, 1054–1060.
(34) Patel, R.N.; Singh, N.; Gundla, V.L.N. *Polyhedron* **2006,** *25*, 3312–3318.
(35) Chandra, S.; Sangeetika, W.; Thakur, S. *Transition Met. Chem.* **2004,** *29*, 925–935.
(36) Symons, M.C.R.; West, D.X.; Wilkinson, J.G. *J. Chem. Soc. Dalton Trans*. **1975,** *16*, 1996–1700.
(37) Rudley, R.J.; Hathaway, B.J. *J. Chem. Soc*. **1970,** *10*, 1725–1728.
(38) Hathaway, B.J.; Billing, D.E. *Coord. Chem. Rev*. **1970,** *5*, 143–207.
(39) Chikate, R.C.; Belapure, A.R.; Padhye, S.B.; West, D.X. *Polyhedron* **2005,** *24*, 889–899.
(40) West, D.X. *Inorg. Nucl. Chem*. **1981,** *43*, 3169–3174.
(41) Malmstrom, B.G.; Vanngard, T. *J. Mol. Biol*. **1960,** *2*, 118–124.
(42) Patterson, G.S.; Holm, R.H. *Bioinorg. Chem.* **1975,** *4*, 1257–1275.
(43) Franco, E.; Lopez-Torres, E.; Mendiola, M.A.; Sevilla, M.T. *Polyhedron* **2000,** *19*, 441–445.
(44) Bu, X.H.; Cao, X.; An, D.L.Ch.; Zhang, R.H.; Thomas, C.; Kimura, E. *J. Inorg. Chem. Soc. Dalton Trans.* **1998,** *3*, 433–437.
(45) Bielski, B.H.J.; Shiue, G.G.; Bajuk, S. *J. Phys. Chem.* **1980,** *84*, 830–833.
(46) Pasternack, R.F.; Halliwell, B. *J. Am. Chem. Soc*. **1979,** *101*, 1026–1031.
(47) Liao, Z.-R.; Zheng, X.-F.; Luo, B.-S.; Shen, L.-R.; Li, D.-F.; Liu, H.-L.; Zhao, W. *Polyhedron* **2001,** *20*, 2813–2821.
(48) Patel, R.N.; Gundla, V.L.N.; Patel, D.K. *Indian J. Chem*. **2008,** *47A*, 353–360.
(49) Han, J.; Xing, Y.; Wang, C.; Hou, P.; Bai, F.; Zeng, X.; Zhang, X.; Ge, M. *J. Coord. Chem*. **2009,** *62*, 745–751.
(50) Bhirud, R.G.; Shrivastava, T.S. *Inorg. Chim. Acta* **1991,** *179*, 125–130.
(51) Simoncini, F.; Rangone, R.; Calanni, C. *Farmaco, Edizione, Pratica, Prat.* **1968,** *23*, 559–570.
(52) Kotschy, A.; Farago, J.; Csampai, A.; Smith, D.M. *Tetrahedron* **2004,** *60*, 3421–3425.
(53) Giugliarelli, G.; Cannistraro, S. *Nuovolimento* **1984,** *4D*, 194–205.
(54) Gray, H.B.; Ballhausen, C.J. *J. Am. Chem. Soc.* **1963,** *85*, 260–265.